PHILOSOPHICAL TRANSACTIONS OF THE ROYAL SOCIETY A MATHEMATICAL, PHYSICAL & ENGINEERING SCIENCES

On the roll–coupling instabilities of high–performance aircraft

Craig C. Jahnke

Phil. Trans. R. Soc. Lond. A 1998 **356**, 2223-2239
doi: 10.1098/rsta.1998.0271

THE ROYAL SOCIETY

On the roll-coupling instabilities of high-performance aircraft

By Craig C. Jahnke

Department of Mechanical, Aerospace and Manufacturing Engineering, Polytechnic University, Brooklyn, NY 11201, USA

High-performance aircraft configurations, characterized by a small span and swept wings, have rolling moments of inertia that are significantly smaller than the pitching or yawing moments of inertia. As a result, nonlinear coupling during high-roll-rate manoeuvres produces significant yawing and pitching moments. For certain critical flight conditions, inertial coupling causes jump phenomena called roll-coupling instabilities. These jump phenomena typically occur as a result of turning-point bifurcations of the aircraft steady states. Analysis of the moment balances along the steady solution branches provides physical insight into the causes of these instabilities and potential means of eliminating them. Analysis performed by using the full eight-degree-of-freedom equations of motion shows that the critical control-surface deflections are essentially the same as for the fifth- and sixth-order equations of motion. Solving the full eight-degree-of-freedom equations allows one to determine the orientation of the aircraft before and after the instability. For the aircraft model studied here, roll-coupling instabilities result in a change in sign of the angle of attack of the aircraft. The equilibrium state of the aircraft changes from a spiral dive, with the bottom of the aircraft closest to the axis of the spiral, to a spiral dive where the top of the aircraft is nearest the axis of the spiral, or vice versa depending on the trim angle of attack from which the manoeuvre was initiated. Pitching moment balance is shown to be central to the instability.

Keywords: instability, roll-coupling; bifurcation; aircraft; dynamics; control loss

1. Introduction

Nonlinear flight dynamics became important with the introduction of high-speed, highly manoeuvrable pursuit aircraft in the 1940s. Inertial coupling of lateral and longitudinal motions during high-speed rolls resulted in instabilities that caused large deviations in sideslip. Large vertical tail loads occurred as a consequence of the excessive sideslip resulting in structural failure of the tails on several aircraft. The first successful analysis of this phenomenon by Phillips (1948) showed that aircraft with low inertia in roll could experience inertial instabilities in pitch or yaw for certain critical roll rates. Subsequent work (Stone 1953; Rhoads & Schuler 1957; Welch & Wilson 1957; Westerwick 1957; Pinsker 1958) focused on calculating the maximum tail loads experienced during roll-coupling instabilities by performing time simulations of aircraft manoeuvres.

By using simplified equations of motion, Gates & Minka (1959) were the first to show that roll-coupling instabilities resulted in the aircraft jumping from one steady flight condition to another. Hacker & Oprisiu (1974) used perturbation analysis to

show that gravity had a small effect on roll-coupling instabilities. Schy & Hannah (1977) and Young *et al*. (1980) went on to analyse the pseudo-steady states of an aircraft. Pseudo-steady states are steady solutions to the equations of motion for an aircraft where the roll angle is assumed to be zero, and the pitch angle and aircraft speed are fixed constant values. These approximations allow one to solve for equilibrium solutions while maintaining the important nonlinearities in angle of attack and roll rate. This work showed that the jump phenomenon occurred as a control-surface deflection was varied past some critical value beyond which the initial steady solution ceased to exist, i.e. at a turning-point bifurcation of the pseudo-steady states. Thus the instability could be predicted and, more importantly, avoided by instructing pilots to avoid critical control-surface deflections.

The availability of continuation methods (Keller 1977) made it possible to calculate the steady solutions of the complete equations of motion, including a nonlinear aerodynamic model. It was now possible to study not only roll-coupling instabilities, where nonlinearities due to inertial coupling are important, but also stall/spin divergence where both inertial coupling and nonlinear aerodynamics are important. Carroll & Mehra (1982), Guichteau (1982, 1990), Planeaux (1988), Planeaux *et al*. (1990) and Jahnke & Culick (1988, 1994) used continuation methods to analyse the steady and/or limit cycle solutions of model jet fighter aircraft. Jahnke & Culick (1988) analysed roll-coupling instabilities of a model fighter aircraft by using a continuation technique to determine the steady solutions of the sixth-order equations of motion. Critical control-surface deflections at which the instabilities occurred were determined and related to Hopf and turning-point bifurcations.

In this paper, roll-coupling instabilities are revisited. The details of the moment balance in the steady solutions are examined to develop an understanding of the cause of the jump phenomenon. Additionally, the change in orientation of the aircraft as a result of the instability is examined by studying the full eight-degree-of-freedom (eight-DOF) equations of motion. The roll-coupling instability is shown to cause the aircraft to go from spiral dive, where the aircraft bottom is closest to the spiral axis, to a spiral dive where the aircraft top is closest to the axis of the spiral, or vice versa. Comparisons with previous results from the fifth- and sixth-order equations of motion show that the critical control-surface deflections are virtually identical for fifth-, sixth- and eight-order equations of motion.

2. Model of aircraft dynamics

The equations of motion used in this work assume a rigid aircraft and constant atmospheric density. In a principal axis system, the equations can be written,

$$\dot{p} = \frac{I_y - I_z}{I_x} qr + \frac{\ell}{I_x}, \tag{2.1}$$

$$\dot{q} = \frac{I_z - I_x}{I_y} pr + \frac{m}{I_y}, \tag{2.2}$$

$$\dot{r} = \frac{I_x - I_y}{I_z} pq + \frac{n}{I_z}, \tag{2.3}$$

$$\dot{\alpha} = q - (p\cos\alpha + r\sin\alpha)\tan\beta + \frac{1}{MV\cos\beta}(Z\cos\alpha - (X+T)\sin\alpha) + \frac{g}{V\cos\beta}(\sin\alpha\sin\theta + \cos\alpha\cos\theta\cos\phi), \tag{2.4}$$

$$\dot{\beta} = p\sin\alpha - r\cos\alpha + \frac{1}{MV}(Y\cos\beta - ((X+T)\cos\alpha + Z\sin\alpha)\sin\beta) + \frac{g}{V}(\cos\alpha\sin\beta\sin\theta + \cos\beta\cos\theta\sin\phi - \sin\alpha\sin\beta\cos\theta\cos\phi), \tag{2.5}$$

$$\dot{V} = \frac{1}{M}(((X+T)\cos\alpha + Z\sin\alpha)\cos\beta + Y\sin\beta) + g(\sin\beta\cos\theta\sin\phi - \cos\alpha\cos\beta\sin\theta + \sin\alpha\cos\beta\cos\theta\cos\phi), \tag{2.6}$$

$$\dot{\theta} = q\cos\phi - r\sin\phi, \tag{2.7}$$

$$\dot{\phi} = p + (q\sin\phi + r\cos\phi)\tan\theta, \tag{2.8}$$

$$\dot{\psi} = (q\sin\phi + r\cos\phi)\sec\theta. \tag{2.9}$$

Note that the yaw angle, ψ, does not appear on the right-hand side of any of the equations of motion, so steady states are determined from equations (2.1)–(2.8) by setting the time derivatives to zero and solving the resulting algebraic equations. In general, the yaw angle will vary with time for an aircraft steady state, since the only possible steady solutions represent either purely longitudinal flight (no lateral motion), or, more generally, flight along a helical flight path where the yaw angle (i.e. heading) changes with time.

Often the effect of gravity is neglected in studies of aircraft dynamics by simply setting g to zero in equations (2.4)–(2.6). The Euler angles (θ, ϕ, ψ) are then decoupled from equations (2.1)–(2.6), and one is left with a reduced set of equations of motion. Since the velocity of the aircraft will not be quantitatively correct without the acceleration of gravity, a constant flight speed is often specified and equations (2.1)–(2.5) are used to simulate the aircraft motion. This gives a fifth-order system of differential equations for the state of the aircraft, and one can determine the thrust required to maintain this speed from equation (2.6). The other option is to specify a constant thrust and solve for the velocity as a function of time knowing there will be some error as a result of neglecting gravity (i.e. the weight of the aircraft).

The aerodynamic model used in this study was obtained from Young *et al.* (1980) and has the form,

$$X = QS(C_X(\alpha) + \delta e C_{X_{\delta e}}(\alpha)),$$

$$Y = QS\left(\beta C_{Y_\beta}(\alpha) + \delta a C_{Y_{\delta a}}(\alpha) + \delta r C_{Y_{\delta r}}(\alpha) + \frac{b}{2V}(pC_{Y_p}(\alpha) + rC_{Y_p}(\alpha))\right),$$

$$Z = QS(C_Z(\alpha) + \delta e C_{Z_{\delta e}}(\alpha)),$$

$$\ell = QSb\left(\beta C_{\ell_\beta}(\alpha) + \delta a C_{\ell_{\delta a}}(\alpha) + \delta r C_{\ell_{\delta r}}(\alpha) + \frac{b}{2V}(pC_{\ell_p}(\alpha) + rC_{\ell_r}(\alpha))\right),$$

$$m = QSc\left(C_m(\alpha) + \frac{c}{2V}qC_{m_q}(\alpha) + \delta e C_{m_{\delta e}}(\alpha)\right),$$

$$n = QSb\left(\beta C_{n_\beta}(\alpha) + \delta a C_{n_{\delta a}}(\alpha) + \delta r C_{n_{\delta r}}(\alpha) + \frac{b}{2V}(pC_{n_p}(\alpha) + rC_{n_r}(\alpha))\right).$$

All aerodynamic coefficients are tabulated for angles of attack from −10 to 90° in increments of 5°. The continuation method used here requires all functions to have continuous first derivatives, so the tabulated data were fitted with cubic splines with tension. The aerodynamic model is linear in sideslip angle, so results will only be valid for sideslip angles between ±10° at most. Also note that no compressibility effects are included in the aerodynamic model. Atmospheric density was assumed to be constant and equal to 0.237 kg m^{-3} and the thrust-to-weight ratio was set to 0.12 for all results presented here.

3. Results and discussion

(a) *Multiple steady solution branches*

A fundamentally important characteristic of nonlinear dynamical systems, such as the equations of motion for an aircraft, is that multiple solutions can exist for specified parameter values. These solutions may be steady states, limit cycles, or aperiodic (e.g. chaotic) motions. Multiple solutions are the norm for most aircraft over the entire range of control surface and thrust settings. For example, spin modes often coexist with desirable manoeuvring and cruising flight conditions. Aircraft instabilities often result in transitions from one solution to another as bifurcations lead to the disappearance of a desired flight condition or cause it to become unstable. As a result, the aircraft enters a new flight condition that can be undesirable or even dangerous.

The current aircraft model possesses several equilibrium states for given control surface and thrust settings. Figure 1 presents the steady solutions of the eighth-order equations of motion as a function of elevator deflection for zero aileron and rudder deflections. These steady solutions were determined with a continuation method based on the work of Doedel & Kernevez (1985). Continuation techniques determine branches of solutions as a function of one parameter of the system, but an initial solution is needed as a starting point. It is often difficult to determine the steady solutions of a nonlinear system of equations such as the equations of motion for an aircraft, and it is usually impossible to prove that all possible steady solutions have been determined.

Stable steady solutions can often be determined with time simulations, but if multiple stable solutions exist, the solution that is eventually approached depends on the chosen initial condition. It is not feasible to try all possible initial conditions, so one could miss stable steady solution branches. Unstable solution branches cannot be found with a time simulation, making it even more difficult to find branches of unstable solutions. Since the aircraft will not enter an unstable flight condition in flight, one may be tempted to dismiss the importance of unstable solutions, but this would be an error for several reasons. First, an unstable solution may become stable as the control-surface deflections or other system parameters are varied. Transient behaviour can also be strongly affected by unstable steady solutions. For example, limit cycles often involve the system oscillating around an unstable steady solution. Wing rock is an example of this, as can be seen by plotting a phase diagram of a wing-rock oscillation (e.g. α versus β) and including the trim condition on the phase plot. Examples of this behaviour can also be found in books on dynamical systems theory (e.g. Guckenheimer & Holmes 1983). More complicated oscillations can occur when the system oscillates around multiple unstable steady solutions (Jahnke *et al.*

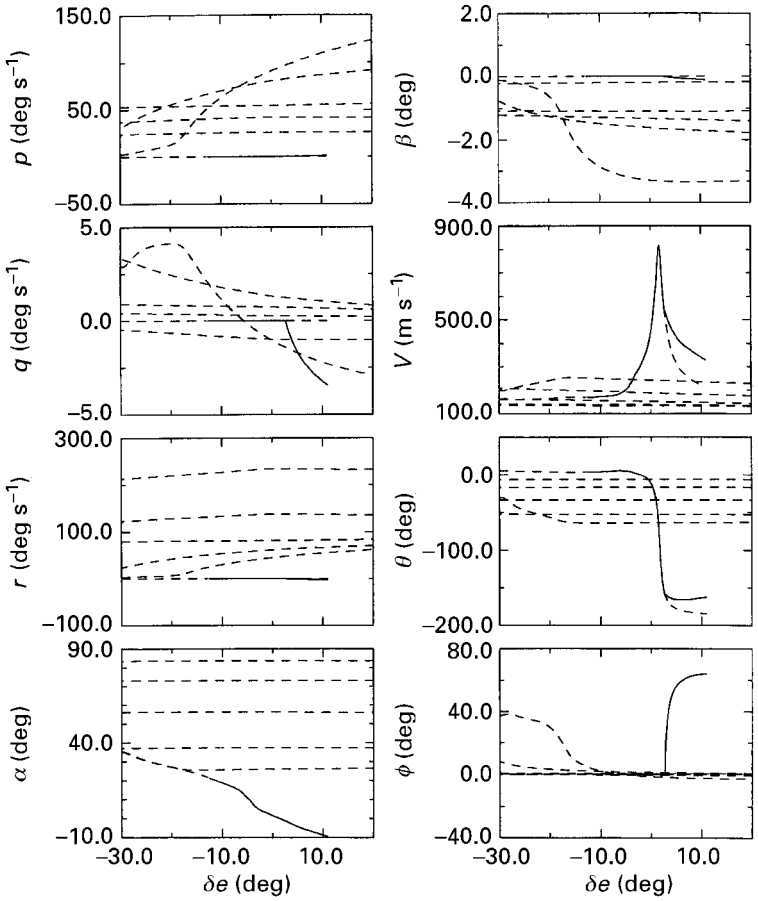

Figure 1. Steady states for $\delta a = 0$, $\delta r = 0$: ——, stable; – – –, unstable.

1998). Typically, a steady solution has several stable linear modes and one or more unstable linear modes. Then the system may approach the unstable steady state in a stable direction, but eventually will leave the vicinity of the unstable steady solution in the unstable direction. Thus, the knowledge of the unstable steady solutions can provide insight into the physics of the motion. In this report, only steady solutions will be discussed, but complicated oscillations have been found to occur for high-performance aircraft (Planeaux *et al*. 1990).

Initial steady solutions for this work were found by using the iteration routine of Young *et al*. (1980) on the fifth-order equations of motion. Gravity was then used as a continuation parameter to connect these pseudo-steady states, where gravity is neglected, to solutions of the full eighth-order equations of motion. All solutions of the fifth-order equations of motion were connected to equivalent solutions in the full equations of motion. This technique provided six of the solution branches in figure 1. Since the equations of motion and the aircraft model is symmetric in the lateral variables, only the positive roll-rates solutions are presented in figure 1. Thus, the solution branches for p, r, β, and ϕ are symmetric about zero while the longitudinal variables (q, α, V, θ) are the same on the symmetric branches. This aircraft then has at least 11 steady solutions (one on the trim branch and on each of five symmetric

branches) for an elevator deflection of, say, $-10°$. This can be seen by counting the number of times a vertical line representing $\delta e = -10$ intersects a steady solution branch taking into account the symmetric counterparts not present in figure 1.

Stable wings level trimmed flight is seen to exist for elevator deflections between -15 and $+3°$, or equivalently, between angles of attack of -3 and $+25°$. The aircraft loses stability at a Hopf bifurcation near an angle of attack of 25°, where this aircraft loses directional stability (i.e. C_{n_β} becomes negative). Steady solution branches with non-zero lateral motions represent spiral and spin modes for this aircraft as illustrated by the large yaw rates. All of the spin modes are unstable for this aircraft model, but the model does not include aerodynamic nonlinearities as a function of the yaw rate so the predicted spin modes are not likely to be physically relevant. As discussed by Chambers *et al.* (1969), if one hopes to simulate the spin modes of an aircraft, it is necessary to include the nonlinear aerodynamic yawing moments that occur at high yaw rates. Rotary balance data are often used for this purpose, but it has proved difficult to obtain wind tunnel data that match full-scale aircraft aerodynamics. Mach number effects are not included in the aerodynamic model used here, so the steady solutions representing high-speed dives are most likely not quantitatively correct. One must always be careful to remember that the results of an analysis are only as good as the model and accurate aerodynamic models for full-scale aircraft are extremely difficult to obtain.

The six steady solution branches discussed above are qualitatively similar for the five-, six- and eight-DOF systems (cf. Young *et al.* 1980; Jahnke & Culick 1988). The largest difference is in the velocity of the aircraft, where one would expect there to be some differences as a result of neglecting the contribution of the aircraft weight. In particular, the dive the aircraft enters for elevator deflections greater than zero cannot be predicted if gravity is neglected. As a result, the pitchfork bifurcation that occurs near an elevator deflection of 3°, where the aircraft becomes inverted, does not occur if gravity is neglected. The pitchfork bifurcation gives rise to a symmetric pair of solutions that represent inverted spirals.

The current aerodynamic model is symmetric in the lateral variables, but this would not be true for a real aircraft. Inevitable asymmetries would be introduced due to the production process or the asymmetric placement of external devices such as probes, fuel tanks, or weapons. This would lead to an unfolding of the pitchfork bifurcation, resulting in a separate branch of solutions unconnected to the primary solution branch. The unconnected branch of solutions would disappear at a critical elevator deflection in a turning-point bifurcation, but where this bifurcation occurs would depend on the degree of asymmetry in the system. Thus, it is important to model the aerodynamics of the actual aircraft as closely as possible. Again, the results of the analysis are only as good as the model of the aircraft.

(*b*) *Roll-coupling instabilities*

Roll-coupling instabilities occur during manoeuvres involving high roll rates, where inertial coupling becomes appreciable; i.e. the terms $((I_z - I_x)/I_y)pr$ in the pitching moment equation and $((I_x - I_y)/I_z)pq$ in the yawing moment equation become significant in the moment balance. For typical high-performance aircraft, I_x is significantly smaller than I_y and I_z as a result of the mass of the aircraft being concentrated along the fuselage due to the typical small span, highly swept wings. For the present

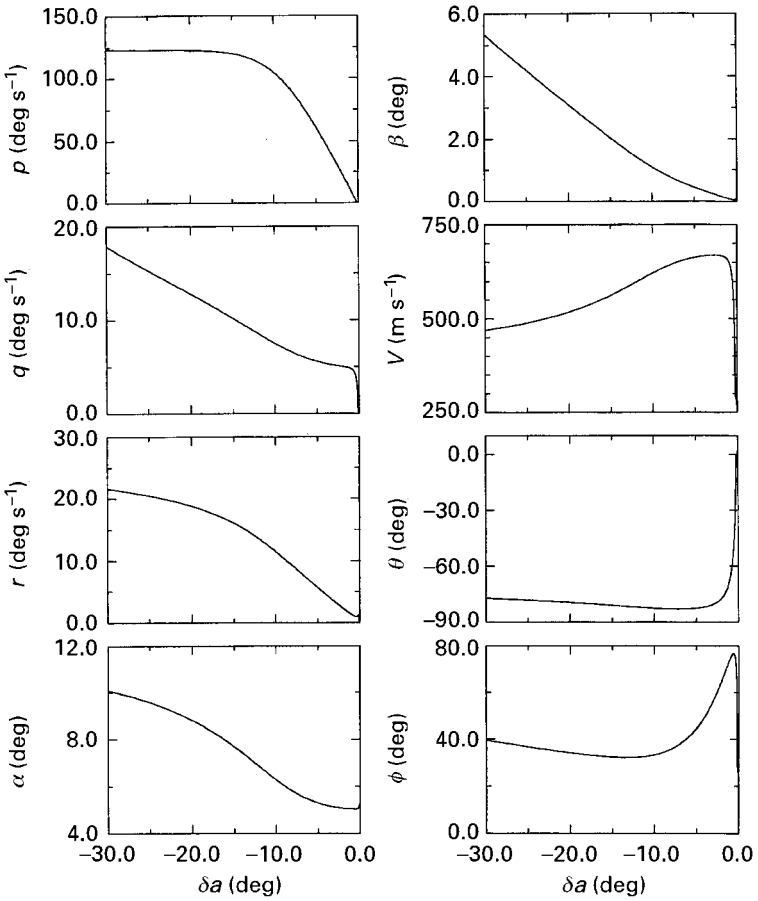

Figure 2. Steady states for $\delta e = -3$, $\delta r = 0$: ——, stable; – – –, unstable.

aircraft model $I_x = 35\,398\ \mathrm{kg\,m^2}$, $I_y = 157\,576\ \mathrm{kg\,m^2}$ and $I_z = 178\,460\ \mathrm{kg\,m^2}$. Note that I_y and I_z are typically close in value, so inertial coupling produces relatively small rolling moments. Also, for a manoeuvring aircraft the roll rate is large while the pitch and yaw rates are substantially smaller so the predominant inertial coupling is for large roll rates to produce significant pitch and yaw moments through inertial coupling.

Figure 2 shows the steady states for rolls from the trim condition at an elevator deflection of $-3°$. Since the aerodynamic model is symmetric in the lateral variables and the aileron deflection, only positive roll-rate solutions are shown. Lateral variables (p, r, β, ϕ) are anti-symmetric, while longitudinal variables (q, α, V, θ) are symmetric in the aileron deflection, along curves of steady solutions. The roll response of this aircraft is good; the steady roll rate increases linearly with aileron deflection for aileron deflections up to $10°$, where the roll rate has reached $100°\ \mathrm{s^{-1}}$. For aileron deflections larger than $10°$ the roll rate is relatively constant, most likely as a result of the opposing moment caused by dihedral effect when the sideslip becomes appreciable. Moderate pitch and yaw rates also build up as the aileron deflection is increased.

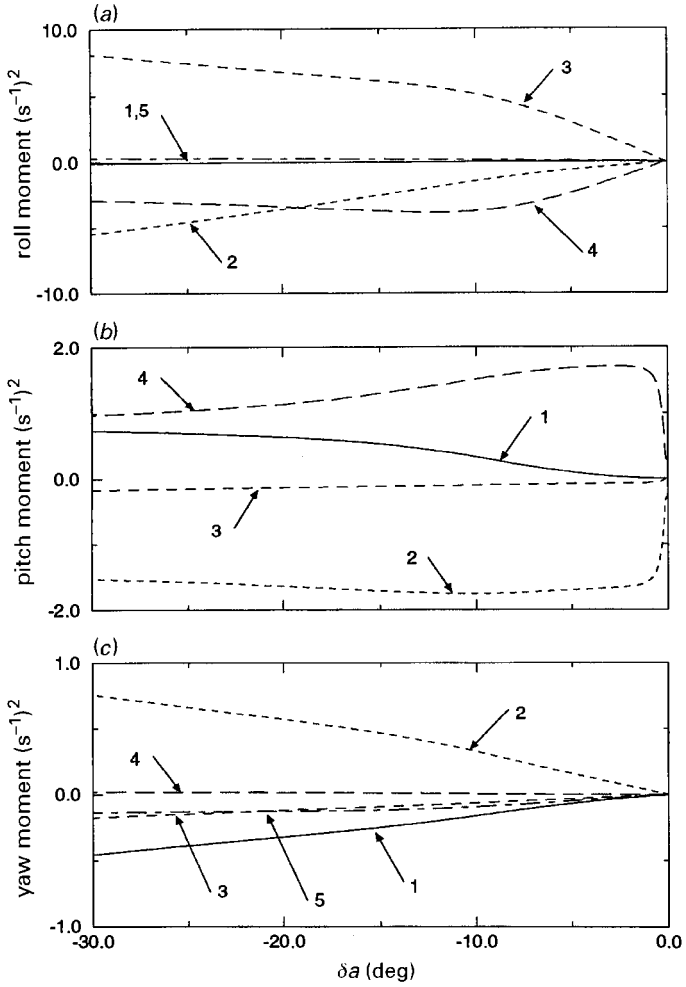

Figure 3. Moment balance in steady states for $\delta e = -3$, $\delta r = 0$. (*a*) $1-(I_y-I_z)qr/I_x$, $2-\beta\ell_\beta/I_x$, $3-\delta a\ell_{\delta a}/I_x$, $4-p\ell_p/I_x$, $5-r\ell_r/I_z$. (*b*) $1-(I_z-I_x)pr/I_y$, $2-m(\alpha)/I_y$, $3-qm_q/I_y$, $4-\delta em_{\delta e}/I_y$. (*c*) $1-(I_x-I_y)pq/I_z$, $2-\beta n_\beta/I_x$, $3-\delta an_{\delta a}/I_x$, $4-pn_p/I_x$, $5-rn_r/I_x$.

Since the full eight-DOF equations of motion are solved, the orientation of the aircraft can be described. Small aileron deflections cause the steady-state orientation of the aircraft to change significantly. For aileron deflections of more than a few degrees, the aircraft pitches down to a pitch angle near $-80°$. Large roll angles and a drastic increase in velocity also occur as the aircraft enters a spiral dive. The large velocity in the dive means that a realistic aerodynamic model would need to include Mach number effects, which are not included in the current model.

It was mentioned above that the roll rate most likely saturates as a result of sideslip build up and the dihedral effect. This can be seen to be the case by examining figure 3, which shows the various terms in the moment balances about each aircraft axis. For small aileron deflections the roll moment due to aileron deflection $(3-\delta a\ell_{\delta a})$ is balanced by damping in roll $(4-p\ell_p)$. Pitching moment balance is achieved by changing the angle of attack (curve 2) to balance the moment created by the elevator

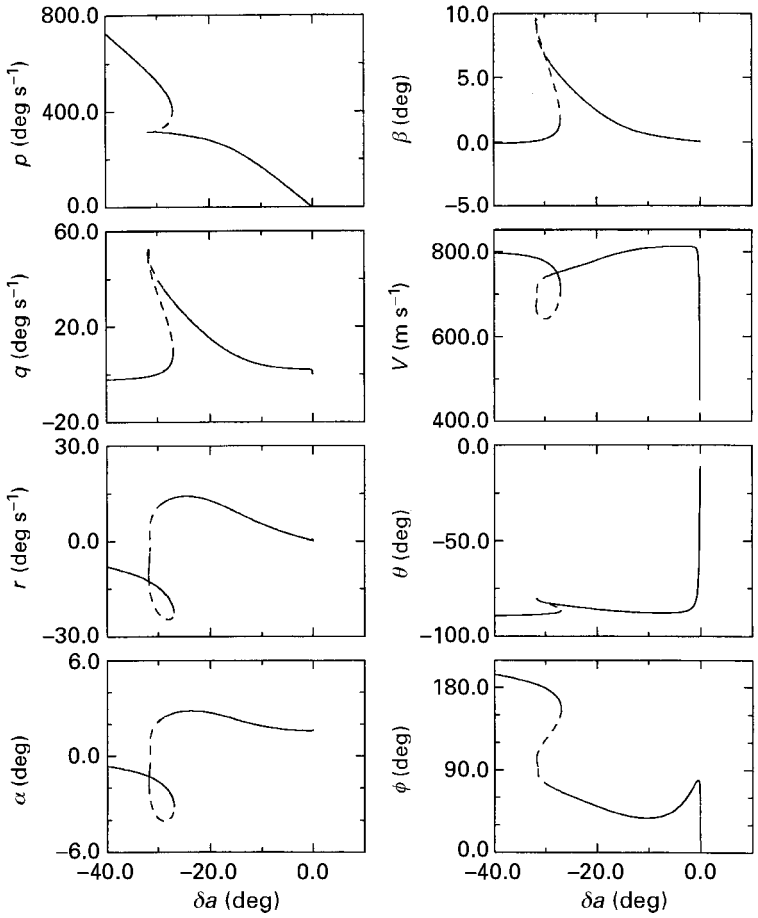

Figure 4. Steady states for $\delta e = 0$, $\delta r = 0$: ——, stable; – – –, unstable.

deflection (curve 4). Yawing moment balance is mainly between the dihedral effect $(2 - \beta n_\beta)$ and inertial coupling with smaller contributions from aileron deflection and damping in yaw. Since inertial coupling becomes stronger with increasing roll rate, sideslip increases with increasing aileron deflection so the directional stability is sufficient to balance the inertial coupling moment. The sideslip then acts to kill the roll through the dihedral effect (see figure 3*a*). Inertial coupling also produces appreciable nose-up pitching moments for large aileron deflections. Even though no instability occurred due to inertial coupling, it has a strong influence on the aircraft motion as it tends to diminish the maximum roll rate of the aircraft.

Roll-coupling instabilities are found to occur for this aircraft for rolls initiated from small or negative angles of attack. Figure 4 shows the steady solutions for rolls initiated from a trim angle of attack of 1.7° ($\delta e = 0$). For aileron deflections less than 25°, figure 4 closely resembles figure 2. For small aileron deflections, the aircraft enters a spiral dive and the roll rate increases linearly for aileron deflections up to 20°, but saturates for larger aileron deflections. A turning-point bifurcation is found to occur at an aileron deflection near 30°. This turning point will cause a jump in the state of the aircraft if the aileron deflection is increased past the critical value evincing

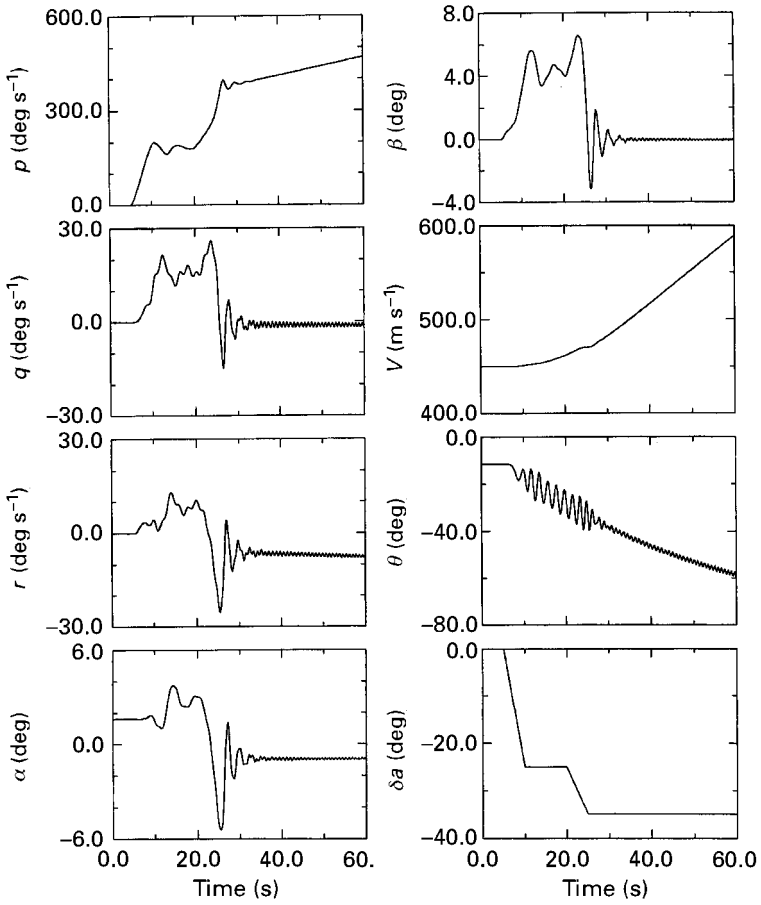

Figure 5. Time simulation of roll-coupling instability for $\delta e = 0$, $\delta r = 0$.

behaviour characteristic of roll-coupling instabilities. One cannot predict the final state of the aircraft after the jump as the aircraft could enter any stable condition, such as a new steady state, a limit cycle or some aperiodic motion. Knowledge of the steady solutions allows one to predict the occurrence of instabilities, but time simulations are necessary to predict the effect of the instability on the aircraft. The details of the manoeuvre in which the instability is encountered may influence the final state of the aircraft if multiple stable motions exist for the final control-surface deflections of the aircraft.

Figure 5 shows a time simulation of the aircraft undergoing a roll-coupling instability by increasing the aileron deflection beyond the critical value at which the turning-point bifurcation occurs. Initially, the aileron deflection is increased to 25°, a deflection less than the critical value. No instability occurs as the aircraft approaches the steady solution. Large jumps are seen to occur in the rotation rates of the aircraft and the sideslip angle between times of 20 and 25 s, where the aileron deflection is increased past the critical value. The angle of attack only changes a few degrees as a result of the instability, but more importantly the angle of attack changes sign. Thus the aircraft goes from a spiral motion where the top of the aircraft faces the axis of

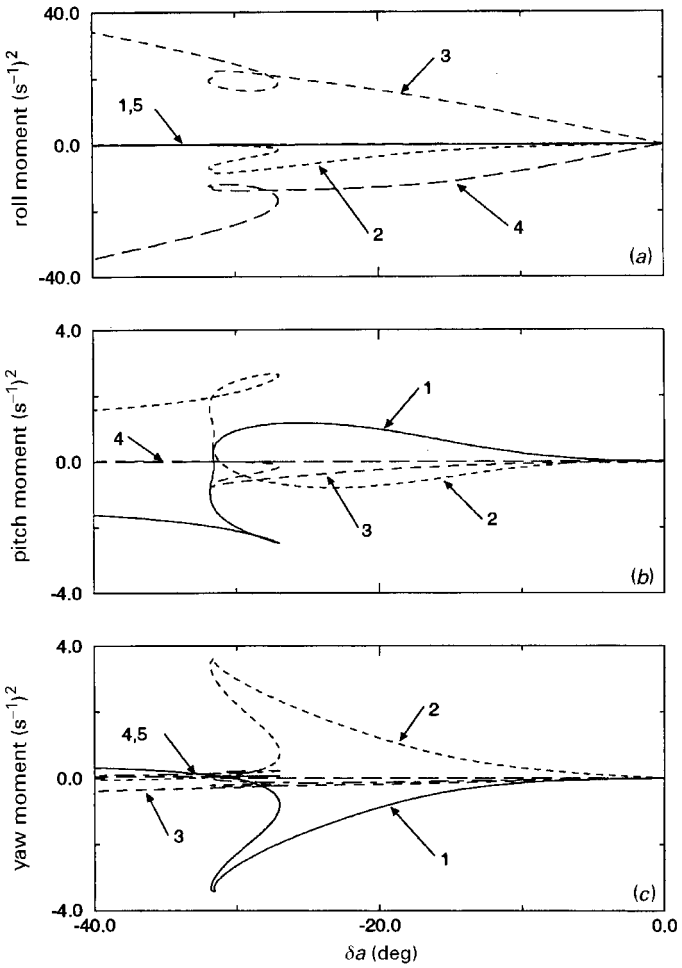

Figure 6. Moment balance in steady states for $\delta e = 0$, $\delta r = 0$. (*a*) $1-(I_y-I_z)qr/I_x$, $2-\beta\ell_\beta/I_x$, $3-\delta a\ell_{\delta a}/I_x$, $4-p\ell_p/I_x$, $5-r\ell_r/I_z$. (*b*) $1-(I_z-I_x)pr/I_y$, $2-m(\alpha)/I_y$, $3-qm_q/I_y$, $4-\delta em_{\delta e}/I_y$. (*c*) $1-(I_x-I_y)pq/I_z$, $2-\beta n_\beta/I_x$, $3-\delta an_{\delta a}/I_x$, $4-pn_p/I_x$, $5-rn_r/I_x$.

the spiral to one where the bottom of the aircraft faces the axis of the spiral as can be deduced from the steady-state pitch and roll angles. Eventually, the aircraft enters the steady state represented in figure 4 that occurs at the final aileron deflection of 35°. The simulation results are shown for a shorter period of time so the details of the instability can be seen. It takes a relatively long time for the velocity and pitch angles to reach their final values while the other variables quickly approach the equilibrium values. The roll rate initially increases very quickly as a result of the instability, but is slow to reach the equilibrium value because the damping due to roll rate depends on the velocity of the aircraft. Note that we may have expected the aircraft to approach this steady state based on figure 4, but one must perform the simulation to be sure as multiple stable motions typically exist for most control-surface deflections.

Further insight into the roll-coupling phenomenon can be gained by examining the moment balance in the steady states. Comparing figures 3 and 6 shows that the

rolling and yawing moment balances are qualitatively the same for the case when roll-coupling instability is absent (figure 3) and when it is present (figure 6). The rolling moment applied by the aileron is balanced by the damping in roll and the dihedral effect, while inertial yawing moments are balanced by directional stability leading to the buildup of sideslip. The pitching moment balance, however, is different for the two cases. For an elevator deflection of 3° (figure 3) the angle of attack is used to balance the pitching moment caused by the elevator. A nose-up moment is created by inertial coupling, but it is not sufficient to change the fundamental pitching moment balance.

For zero elevator deflection (figure 6) no pitching moment is created by the elevator, so the moment balance is between the inertial coupling moment and the moment due to angle of attack. For small aileron deflections the angle of attack grows in response to the stronger inertial coupling that occurs as the roll rate increases (see figure 4). Eventually, the pitch rate grows enough to also help balance the inertial coupling moment. Once the combination of angle of attack and pitch rate are insufficient to balance the inertial moment, the inertial moment must decrease in order to maintain equilibrium. This occurs by decreasing the yaw rate (see figure 4). Near the turning point the yaw rate changes sign causing the inertial pitching moment to change sign. Since the angle of attack is used to balance the inertial pitching moment, the angle of attack must also change sign. Thus the instability is a transition from positive angle of attack flight to negative angle of attack flight, representing the two types of spiral motions described above.

Since the roll-coupling instability discussed above caused the aircraft to go from a steady flight condition with a positive angle of attack to one with a negative angle of attack, one may wonder what occurs if a roll is initiated from a negative angle of attack. Figure 7 shows the steady solutions as a function of aileron deflection with an elevator deflection of 3°, for which the trim angle of attack is −2°. At trim the aircraft is flying inverted with a pitch angle near −165°. Very small aileron deflections cause the aircraft to enter a spiral dive. The pitch angle approaches −90°, the roll angle becomes non-zero and the velocity increases to very large values. A turning-point bifurcation occurs at an aileron deflection of 12° leading to a jump in the state of the aircraft if the aileron deflection is increased past that critical value, again representative of a roll-coupling instability for the aircraft.

Similar to the roll initiated from a positive trim angle of attack, a large jump in roll rate occurs (from 260 to 400° s^{-1}) as a result of the roll-coupling instability while the yaw rate and angle of attack change signs. In this case the angle of attack goes from negative to positive as the aileron deflection is increased past the critical value, indicating that the aircraft has transitioned from a spiral with the bottom of the aircraft towards the axis of the spiral to one where the top of the aircraft faces the axis of the spiral. This is the reverse of the sequence that occurs for rolls initiated from a positive trim angle of attack, but the physics of the instability is equivalent.

Figure 8 shows the moment balances about the aircraft axes in the steady states for an elevator deflection of 3°. Yawing moment balance is again maintained between inertial coupling and the directional stability leading to a build-up in sideslip angle. In the present case negative sideslip occurs, so in the rolling moment balance dihedral effect adds to the moment caused by the aileron resulting in a larger roll rate being necessary to obtain sufficient damping in roll. Thus for a given aileron deflection, the roll rate is larger for rolls initiated from negative angles of attack than for rolls

PHILOSOPHICAL TRANSACTIONS OF THE ROYAL SOCIETY A MATHEMATICAL, PHYSICAL & ENGINEERING SCIENCES

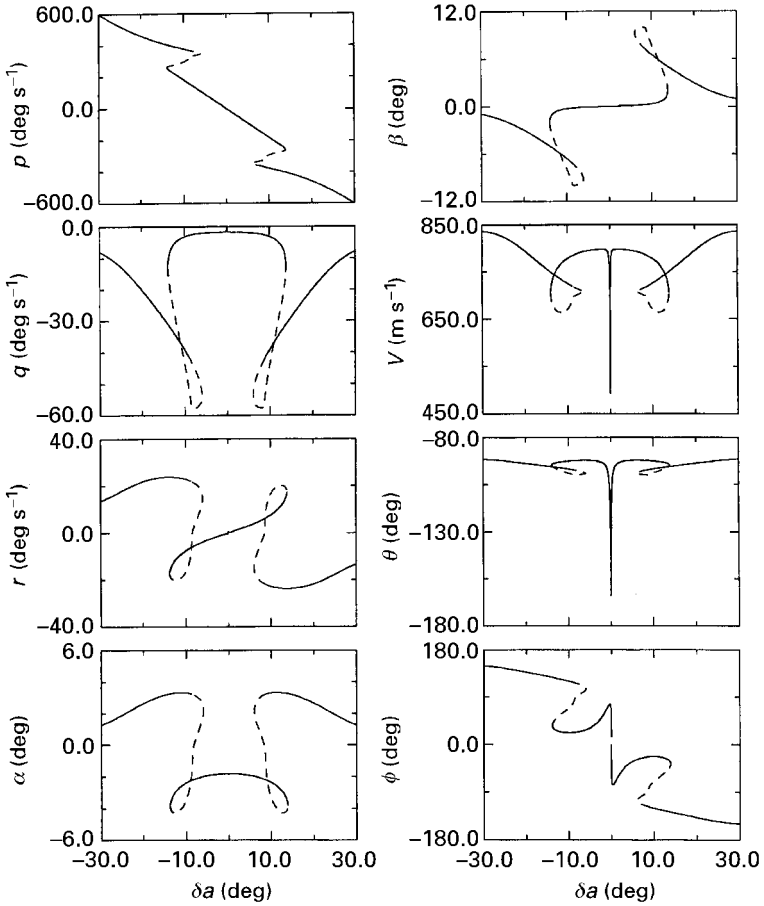

Figure 7. Steady states for $\delta e = 3$, $\delta r = 0$: ——, stable; – – –, unstable.

initiated from positive angles of attack. Physically, this means that for a given aileron deflection spiralling the aircraft, with the bottom of the aircraft towards the axis of the spiral, leads to larger roll rates than when the top of the aircraft is towards the axis of the spiral. The reverse would occur for an aircraft with negative dihedral effect (i.e. $C_{\ell_\beta} > 0$).

The ultimate cause of the roll-coupling instability can again be seen in the pitching moment balance (figure 8*b*). For small aileron deflections, pitching moment balance is maintained between the angle of attack and the elevator deflection. As the inertial coupling moment increases, the angle of attack becomes a larger negative value to maintain the moment balance. When this is not sufficient (i.e. for steady solutions beyond the instability), the moment balance is principally between the effects of elevator deflection and inertial coupling with a smaller contribution from angle of attack. As in the previous case, the sign of the inertial moment changes as a result of the instability, again due to the yaw rate changing signs.

The critical aileron and elevator deflections at which roll-coupling instabilities occur is shown in figure 9. Only the control-surface deflections for positive roll-rate solutions are shown. Negative roll-rate solutions have critical control-surface

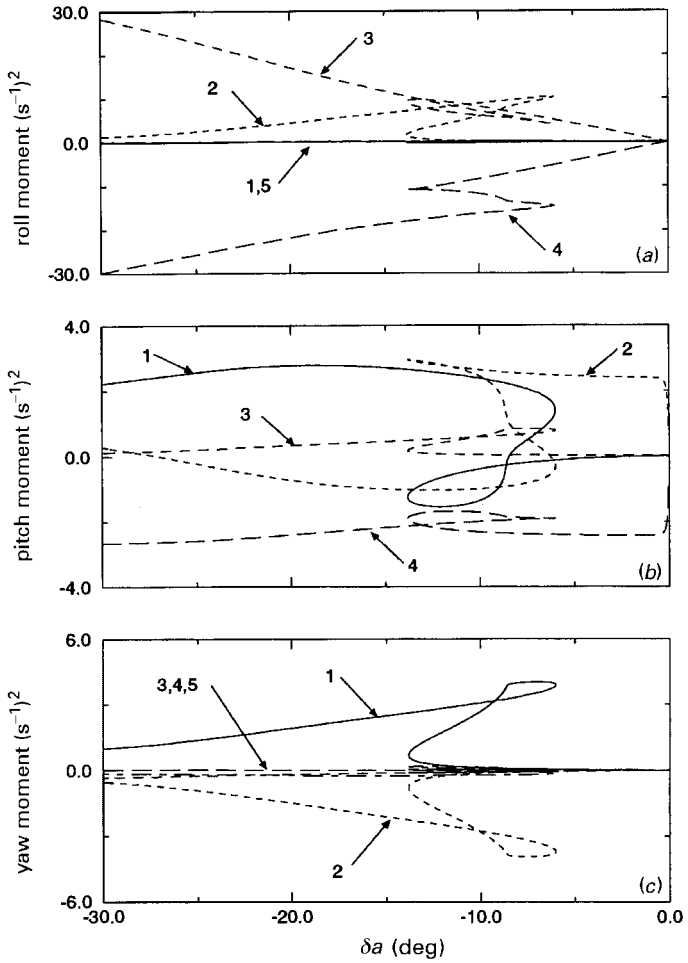

Figure 8. Moment balance in steady states for $\delta e = 3$, $\delta r = 0$. (*a*) $1-(I_y-I_z)qr/I_x$, $2-\beta\ell_\beta/I_x$, $3-\delta a\ell_{\delta a}/I_x$, $4-p\ell_p/I_x$, $5-r\ell_r/I_z$. (*b*) $1-(I_z-I_x)pr/I_y$, $2-m(\alpha)/I_y$, $3-qm_q/I_y$, $4-\delta em_{\delta e}/I_y$. (*c*) $1-(I_x-I_y)pq/I_z$, $2-\beta n_\beta/I_x$, $3-\delta an_{\delta a}/I_x$, $4-pn_p/I_x$, $5-rn_r/I_x$.

deflections of the opposite sign in aileron deflection for the same elevator deflection. That is, the complete figure would have symmetry about zero aileron deflection. The Hopf bifurcations that occur near the turning-point bifurcations are also shown. Note that two regions of instability occur. One region is for rolls initiated from positive trim angles of attack while the other region represents instabilities of rolls initiated from negative angles of attack. These two instabilities are not directly connected as no instability occurs for elevator deflections between 1.0 and 1.5°.

Critical aileron and elevator deflections at which roll-coupling instabilities occur are virtually identical for the fifth-, sixth- and eighth-order equations of motion (cf. Young *et al*. 1980; Jahnke & Culick 1988). Thus gravity does not affect the instability, which is not surprising given the above results which show that the instability arises in the moment balance and gravity does not directly affect the moment on the aircraft. Aircraft flight speed does not affect the critical control-surface deflections

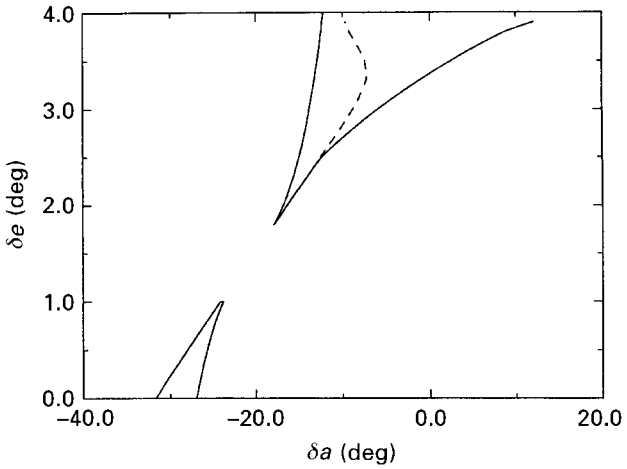

Figure 9. Bifurcation set for roll-coupling instability with $\delta r = 0$: ——, turning point; – – –, Hopf bifurcation.

either, as the fifth-, sixth- and eighth-order equations of motion have different steady velocities. This is an artefact of neglecting compressibility effects, which means that the velocity only affects the dynamic pressure, which cancels out in determining the critical control-surface deflections at which bifurcations occur. The state of the aircraft at the turning point is not the same for the three different systems of equations of motion as the rotation rates scale with the velocity while the angles of attack and sideslip are independent of aircraft speed.

4. Conclusions

Several key aspects of nonlinear aircraft dynamics have been illustrated in this paper. Multiple steady solutions for fixed aircraft parameters are the norm due to the nonlinearity of both the rigid-body equations of motion and aerodynamic models. Typically, more than one steady spin mode exists for an aircraft, and pitchfork and/or turning-point bifurcations can lead to multiple steady solutions. In this paper a pitchfork bifurcation was shown to cause the longitudinal trim condition to become unstable and lead to the emergence of a pair of stable spiral modes. The turning points characteristic of roll-coupling instabilities were shown to lead to jumps in the state of the aircraft if a control-surface deflection was varied past the critical value. Hysteresis may also occur due to the multiple steady solutions that occur between the pair of turning-point bifurcations that arise in the roll-coupling instability.

Use of the full eighth-order equations of motion was shown to be necessary to unravel the physics of roll-coupling instabilities. The instability was only found to occur when the aircraft was in a spiral dive and the instability resulted in a transition from one type of spiral to another. One spiral occurred at negative angles of attack where the aircraft was orientated with the bottom towards the axis of the spiral. The other spiral occurred at positive angles of attack where the top of the aircraft faced the axis of the spiral. Additional details of the instability were discussed in terms of the moment balances in the steady solutions. The pitching moment balance was shown to be the key to the instability as the jump, causing a sign change in angle of

attack, occurred as a result of the need to balance the inertial coupling moment in pitch.

More generally, it was illustrated that using continuation methods for determining steady solutions and time simulations for examining manoeuvres is a very fruitful approach. Maps of steady solutions as functions of the parameters of the aircraft provide a global view of the possible equilibrium solutions. Adding linear stability information shows the equilibrium solutions that the aircraft may exhibit in flight, while changes in stability signify instabilities. This global knowledge allows one to use time simulations to examine interesting or troublesome regions of the flight envelope. Steady solutions can typically be computed faster that time simulations, so the combination of the two techniques has the potential to reduce computational costs. The next step is to compute the basins of attraction of the various equilibrium solutions. One would then be able to predict the final state of an aircraft for a given initial condition. Jahnke & Chen (1995) have taken an initial step in determining basins of attraction of steady solutions, but much work remains to be done.

Funding for this work was provided by the National Science Foundation under Grant no. CMS-9409025.

Appendix A. Nomenclature

α	angle of attack
β	sideslip angle
δa	aileron deflection
δe	elevator deflection
δr	rudder deflection
ϕ	roll angle
θ	pitch angle
ψ	yaw angle
b	wing span
c	mean wing chord
g	acceleration due to gravity
I_x	moment of inertia about aircraft x-axis
I_y	moment of inertia about aircraft y-axis
I_z	moment of inertia about aircraft z-axis
ℓ	aerodynamic rolling moment
m	aerodynamic pitching moment
M	aircraft mass
n	aerodynamic yawing moment
p	roll rate
q	pitch rate
Q	dynamic pressure
r	yaw rate
S	wing surface area
T	applied thrust
V	aircraft speed
X	aerodynamic force along aircraft x-axis
Y	aerodynamic force along aircraft y-axis
Z	aerodynamic force along aircraft z-axis

References

Carroll, J. V. & Mehra, R. K. 1982 Bifurcation analysis of nonlinear aircraft dynamics. *J. Guidance* **5**, 529–536.

Chambers, J. R., Bowman, J. S. & Anglin, E. L. 1969 Analysis of the flat-spin characteristics of a twin-jet swept-wing fighter airplane. NASA TN D-5409.

Doedel, E. J. & Kernevez, J. P. 1985 Software for continuation problems in ordinary differential equations with applications. Preprint, California Institute of Technology.

Gates, O. B. & Minka, K. 1959 Note on a criterion for severity of roll-induced instability. *J. Aerospace Sci.* **5**, 287–290.

Guckenheimer, J. & Holmes, P. 1983 *Nonlinear oscillations, dynamical systems, and bifurcations of vector fields.* New York: Springer.

Guicheteau, P. 1982 Bifurcation theory applied to the study of control losses on combat aircraft. Resch. Aerosp. 2.

Guicheteau, P. 1990 Bifurcation theory in flight dynamics an application to a real combat aircraft. In *ICAS Congress, Stockholm, September 1990*, ICAS paper 90-116.

Hacker, T. & Oprisiu, C. 1974 A discussion of the roll-coupling problem. *Progr. Aerospace Sci.* **15**, 151–180.

Jahnke, C. C. & Chen, G. 1995 Nonlinear stability analysis of aircraft steady states. In *AIAA Atmospheric Flight Mechanics Conf.*, AIAA Paper 95-3449.

Jahnke, C. C. & Culick, F. E. C. 1988 Application of dynamical systems theory to nonlinear aircraft dynamics. In *AIAA Atmospheric Flight Mechanics Conf.*, AIAA Paper 88-4372.

Jahnke, C. C. & Culick, F. E. C. 1994 Application of bifurcation theory to the high angle of attack dynamics of the F-14. *J. Aircraft* **31**, 26–34.

Jahnke, C. C., Subramanyam, V. & Valentine, D. T. 1998 On the convection in an enclosed container with unstable side wall temperature distributions. *Int. J. Heat Mass Transfer* **41**, 2307–2320.

Keller, H. B. 1977 *Numerical solution of bifurcation and nonlinear eigenvalue problems. Applications of bifurcation theory* (359 pp.). New York: Academic.

Phillips, W. H. 1948 Effect of steady rolling on longitudinal and directional stability. NASA TN 1627.

Pinsker, W. J. G. 1958 Critical flight conditions and loads resulting from inertia cross coupling and aerodynamic stability deficiencies. ARC Technical Report CP No. 404.

Planeaux, J. B. 1988 High-angle-of-attack dynamic behavior of a model high performance fighter aircraft. In *AIAA Atmospheric Flight Mechanics Conf.*, AIAA Paper 88-4368.

Planeaux, J. B., Beck, J. A. & Baumann, D. D. 1990 Bifurcation analysis of a model fighter aircraft with control augmentation. In *AIAA Atmospheric Flight Mechanics Conf.*, AIAA Paper 90-2836.

Rhoads, D. W. & Schuler, J. M. 1957 A theoretical and experimental study of airplane dynamics in large disturbance maneuvers. *J. Aeronautical Sci.* **7**, 507–526.

Schy, A. A. & Hannah, M. E. 1977 Prediction of jump phenomena in roll-coupled maneuvers of airplanes. *J. Aircraft* **14**, 375–382.

Stone, R. W. 1953 An estimation of the maximum angle of sideslip for determination of vertical tail loads in rolling maneuvers. NASA Report No. 1136.

Welch, J. D. & Wilson, R. E. 1957 Cross-coupling dynamics and the problem of automatic control in rapid rolls. *J. Aeronautical Sci.* **10**, 741–754.

Westerwick, R. 1957 The roll-coupling problem – a mathematical approach. *Aeronautical Engng Rev.* **12**, 48–51.

Young, J. W., Schy, A. A. & Johnson, K. G. 1980 Pseudo-steady-state analysis of nonlinear aircraft maneuvers. NASA TP 1758.

PHILOSOPHICAL TRANSACTIONS OF THE ROYAL SOCIETY A MATHEMATICAL, PHYSICAL & ENGINEERING SCIENCES